

## Removal of Methylene Blue by Low-Cost Adsorbent Prepared from Jujube Stones – Kinetic and Thermodynamic Studies

Asmae Sanad<sup>1</sup>, Meryem Bensemlali<sup>1</sup>, Badreddine Hatimi<sup>1</sup>,  
Fatima Zahra Chajri<sup>1</sup>, Meryeme Joudi<sup>1,2\*</sup>, Abdellatif Aarfane<sup>1,4</sup>,  
Najoua Labjar<sup>3</sup>, Mina Bakasse<sup>1</sup>, Hamid Nasrellah<sup>1,4</sup>

<sup>1</sup> Laboratory of Organic Bioorganic Chemistry and Environment, Faculty of Sciences, University Chouaib Doukkali, El Jadida, Morocco

<sup>2</sup> Laboratory of Analytic and Molecular Chemistry, Faculty of Sciences Casablanca, Morocco

<sup>3</sup> Laboratory of Spectroscopy, Molecular Modelling, Materials, Nanomaterials, Water and Environnement, ENSAM University Mohammed V in Rabat, Morocco

<sup>4</sup> Higher School of Education and Training, University Chouaib Doukkali, El Jadida, Morocco

\* Corresponding author's e-mail: [joudi.doct@gmail.com](mailto:joudi.doct@gmail.com)

### ABSTRACT

Agricultural residue emerges as a cost-effective and readily available option for the adsorption of dyes, owing to its affordability and efficacy. The purpose of our study focuses on the methylene blue dye (MB) removal using chemically modified jujube stone (MJS) as an adsorbent. The MJS underwent characterization through multiple methodologies including scanning electron microscopy (SEM), Energy dispersive X-ray spectroscopy (EDX), X-ray diffraction (XRD) and Fourier transform infrared spectroscopy (FTIR). The research systematically investigated contact time, PH, temperature, initial dye concentration, and adsorbent dosage impact to optimize the removal efficiency. Experimental findings demonstrated that the MJS adsorbent achieved a dye removal efficiency of approximately 94% under batch mode and room temperature conditions. Kinetic analysis revealed an equilibrium time of around 70 minutes. Remarkably, this study unveils the novel application of chemically customized jujube stone a highly effective adsorbent for removing methylene blue dye. Applying the pseudo-second-order model provides the most precise description for methylene blue (MB) adsorption onto MJS. The modeling of adsorption isotherms indicated conformity to the Langmuir model. The thermodynamic study shows a negative value of  $\Delta G$ , which demonstrates spontaneous MB adsorption into MJS, while a positive value of  $\Delta H$  implies an endothermic adsorption process.

**Keywords:** kinetic, thermodynamic study, methylene blue, adsorption, removal, jujube stones.

### INTRODUCTION

Water is the most invaluable resource for humans (Sahoo and Goswami, 2024). Unfortunately, many industries, such as the textile industry, expends significant quantities of and generate polluted wastewater by adding chemical dyes to color their products (Miranda et al., 2024). These dyes are considered dangerous organic compounds in the environment (Al-Tohamy et al., 2022). Methylene blue

(MB) emerges as a hazardous dye known for its persistence in the environment (Saning et al., 2024). Its presence can lead to significant environmental issues in freshwater reservoirs. Often released into natural water bodies, it directly affects aquatic ecosystems (Venkatesan et al., 2024). Additionally, MB can bioaccumulate in aquatic organisms, potentially increasing contamination levels in the food chain (Bulin et al., 2024). Furthermore, industrial discharges containing MB contribute

to wastewater pollution, posing a threat to aquatic ecosystems (El-Shafie et al., 2024). For this reason, this wastewater needs an effective treatment to mitigate its effects. Unfortunately, the contaminated water issue from textile industries poses a serious environmental concern for development (Gomes et al., 2024). Currently, national and international organizations focus their research on this problem. Hence, various methods have been employed for treating wastewater, such as coagulation-flocculation, chemical oxidation, and adsorption (Shende and Chidambaram, 2024), (Panwar et al., 2024; Vidarth et al., 2024).

Recently, adsorption has been used for its simplicity and cost-effectiveness. Biomaterials derived from organisms and agricultural by-products have been used in several studies for their high adsorption capacity, environmental friendliness, and affordability (Bal, Thakur, 2022; Benjelloun, al., 2021; Nimbalkar, Bhat, 2021; Rashid al., 2021). This study uses waste jujube seeds as an adsorbent to adsorb MB dye. *Ziziphus jujube* is a Mediterranean species used in food and traditional medicine. Its utilization generates a large quantity of undesirable waste that should be valorized. (Ghobadi et al., 2019).

In this research, *Ziziphus jujube* is employed as biomass to prepare a new adsorbent. This adsorbent is prepared with low energy costs by adding a hydroxide solution (NaOH) and phosphoric acid ( $H_3PO_4$ ). The probable adsorption mechanism was described through characterization using FTIR, DRX, and SEM/EDAX.

The objective of this study is to investigate the viability of using discarded jujube seeds as a new adsorbent for eliminating methylene blue dye from wastewater, thereby tackling environmental and economic considerations.

## MATERIALS AND METHODS

### Customized jujube stones preparation

*Ziziphus jujube* stones (JS) were collected from Zagora, Morocco, and rinsed with distilled water. They were dried under the sun, ground, and sieved between 500  $\mu\text{m}$  and 800  $\mu\text{m}$ . The sieved product was heating up within a round-bottom flask with a hydroxide solution of 12% for 4 hours. The filtered product

was stirred with phosphoric acid 67% during 24 hours. Distilled water was used to wash the resulting product until reaching a neutral pH and subsequently dried at 100 °C.

### Equipment and method

The suggested adsorbents underwent characterization using Nicolet IS50 FTIR spectrometer, spanning from 4000 to 600  $\text{cm}^{-1}$ . The SEM-EDX employed in this investigation is a Hirox SH-5500P microscope. The XRD utilized is a Bruker diffractometer with Cu-K $\alpha$  radiation spanning the  $2\theta$ -range of 15–100°. The concentration of MB was measured using VJESCO 370 ultraviolet-visible spectroscopy at a wavelength of 665 nm. The present study uses methylene blue (MB) as an adsorbate. MB is a chemical compound with a heterocyclic aromatic structure (Iwuzor et al., 2021). The molecular formula is  $C_{16}H_{18}N_3SCl$ , and the formula weight is 319.85 g/mol. It's a cationic molecule that is part of the xanthine family. (Narayanan, Jayasundara, 2022; Yang et al., 2024).

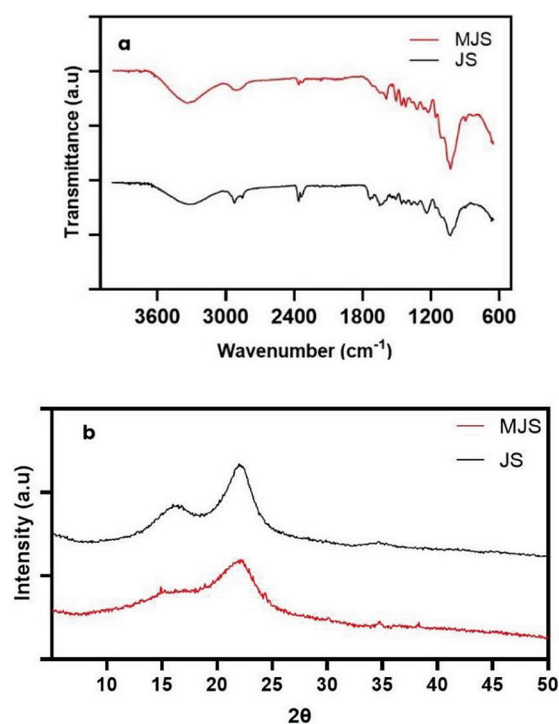


**Figure 1.** FTIR spectra (a), and X-ray diffraction spectra of jujube stone (JS) and modified jujube stone (MJS) (b)

## Batch experiment

The tests were conducted using 100 ml solutions of MB dye at room temperature (25 °C). The MB powder was diluted to prepare the initial concentration of the solutions, which were then brought into contact with a mass of MJS. The mixture was stirred at 500 rpm. Afterward, it was separated from the solid using a centrifuge, and finally, the concentration was quantified.

The efficiency of MB removal (%) and the amount of MB adsorbed ( $Q_t$ ) were obtained using Equations 1 and 2:

$$MB \text{ removal } (\%) = \frac{C_0 - C_e}{C_0} \times 100 \quad (1)$$

$$Q_t = \frac{(C_0 - C_t)}{W} \times V \quad (2)$$

where:  $C_0$ ,  $C_t$  and  $C_e$  represent the concentrations of MB dye at the initial, time and equilibrium states of adsorption (in mg/L), respectively.  $W$  (g) and  $V$  (L) indicate the amount of MJS utilized as an adsorbent and the initial volume of the solution under investigation.

Several variables on the adsorption of MB dye on the MJS surface were investigated, including the duration of contact ranging from 0 to 150 minutes, pH levels spanning from 2 to 11, and initial concentrations of MB dye varying from 10 mg/L to 350 mg/L and the mass of the adsorbent (MJS) ranging from 0.1 to 2.25 g.

## RESULTS AND DISCUSSION

### Characterizations of MJS

#### FTIR characterization

The FTIR analysis, illustrated in Figure 1a, provides insights into the chemical bonds and functional groups found in both (JS) and (MJS). The FTIR spectrum of JS and MJS adsorbents exhibits a prominent and broad band at 3314  $\text{cm}^{-1}$ , indicating –OH vibrations. Additionally, the band observed at 2922  $\text{cm}^{-1}$  relates to the C–H group's symmetrical stretching. Bands at 1729  $\text{cm}^{-1}$  and 1639  $\text{cm}^{-1}$  are related to stretching vibration of C = O and C = C groups, respectively. Furthermore, the band at 1236  $\text{cm}^{-1}$  is attributed to C = C vibration in aromatic rings, while the band centered at 1060  $\text{cm}^{-1}$  is indicative of C–N stretching

vibration (Bouchelkia et al., 2023; Khan et al., 2022a, 2022b; Regti et al., 2017). The band observed at 1162  $\text{cm}^{-1}$  corresponds to corroborated symmetrical vibrations of phosphate (Khan et al., 2022a) resulting from  $\text{H}_3\text{PO}_4$  after modification. The band at 1750  $\text{cm}^{-1}$  is indicative of C = O (Rawat and Garg, 2021). However, the band detected at 2300  $\text{cm}^{-1}$  was assigned to C  $\equiv$  C (Palisoc et al., 2020); with its reduction attributed to the decomposition of cellulose (Shen et al., 2019).

#### X-ray diffraction

XRD is employed for JS and MJS structure identification (Ali et al., 2022). Figure 1b shows wide peaks indicating an amorphous structure. A broad and intense peak is observed around 22–25°. This peak is identical to the (0 0 2) diffraction of graphite. The natural JS displays a distinct peak at  $2\theta = 16.3$ , a peak that disappears entirely in the MJS due to cellulose decomposition. The non-existence of a slim peak indicates that the structure is primarily amorphous (Bouchelta et al., 2008; Sher et al., 2020).

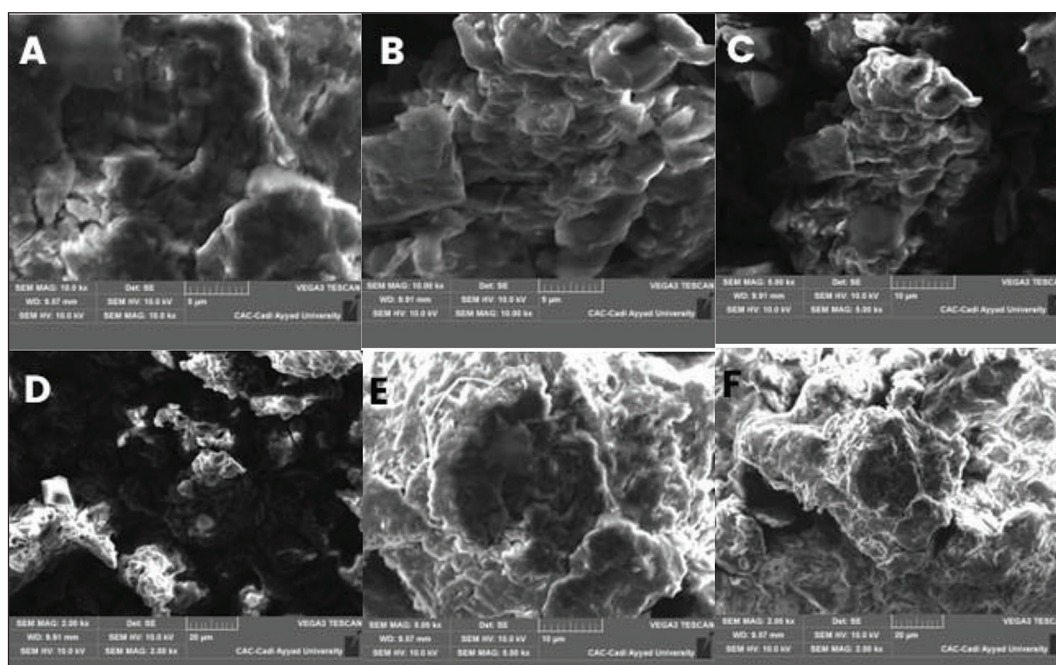
#### SEM characterization

SEM analysis is utilized to investigate the surface properties and structure of both the modified jujube seeds (MJS) and untreated jujube seeds (JS), as well as to conduct elemental analysis utilizing the EDX method (Y. Li et al., 2020) (Figure 2). The obtained images indicate that the particles exhibit irregular pores before and after chemical modification of JS (Hariharana et al., 2023), and the images also show a lamellar texture and considerable roughness, therefore, the functional groups based on carbon are responsible for the roughness on the MJS surface. These characteristics have a lot of benefits, including maximizing the surface area and creating more adsorbable sites. Using  $\text{H}_3\text{PO}_4$  may have enhanced the texture of adsorbent surfaces (Mokhtaryan et al., 2023).

The chemical composition analysis of JS and MJS using energy dispersion X-ray presented in Table 1 illustrates alterations in the compositions and proportions that occurred in ziziphus jujube throughout the chemical modification process. The EDX analysis reveals a decrease in the surface proportion of diverse major elements, such as carbon, oxygen and other trace elements (Figure 3).

**Table 1.** Chemical composition of JS and MJS

Element	JS		MJS	
	Weight %	Atomic %	Weight %	Atomic %
C	64.54	72.52	58.51	65.61
O	30.23	25.50	40.06	33.72
F	0.00	0.00	0.08	0.05
Na	0.18	0.10	0.12	0.07
Mg	0.20	0.11	0.05	0.03
Al	0.15	0.08	0.26	0.13
Si	0.12	0.06	0.05	0.02
P	0.37	0.16	0.72	0.31
S	0.46	0.19	-	-
K	1.40	0.48	-	-
Ca	2.34	0.79	0.16	0.05

**Figure 2.** SEM micrographs of JS 5 $\mu$ m (a), 10 $\mu$ m (b), 20  $\mu$ m (c), and MJS 5  $\mu$ m (d), 10  $\mu$ m (e) 20  $\mu$ m (f)

### Effect of parameters on the adsorption of MB using MJS

#### Contact time effect

Contact time plays a crucial role in dye adsorption efficiency. It has been varied between 0 to 150 minutes in this study. The utilization of MJS as an adsorbent demonstrates an enhancement in MB adsorption efficiency with prolonged contact time. Figure 4a illustrates that adsorption occurred rapidly within the initial 30 minutes and continued to increase as the contact time was extended. After 70 minutes of being in contact, no notable change in the adsorbed dye was observed.

The initial rapid rate might be ascribed to the accessibility of surface sites on the MJS surfaces (Garg et al., 2023).

#### Adsorbent amount effect

Figure 4b illustrates the adsorbent quantity impact, with the MJS amount ranging from 0.1 g to 2.25 g in a 100 ml solution of MB dye, initially set at 15 mg/L concentration, while keeping the rest of the parameter's constant. According to the results, when the dose of MJS is raised up to 0.6 g, the removal percent increases and then approximately stays constant due to the accessibility of MJS sites. Moreover, the adsorption of

MB reaches an equilibrium above 0.6 g. It eventually reached a relatively stable value because of the existence of unoccupied adsorption sites on the adsorbent's surface (Liu et al., 2024).

*pH solution effect*

The initial pH was examined within the range of 2 to 11 by adjusting it with the addition of

HCl or NaOH (H.-Z. Li et al., 2021). The data in Figure 5c demonstrates a strong correlation between the initial pH levels of the solutions and the percentage of MB removed. Optimal pH values for efficient adsorption range from 6 to 11. This trend can be attributed to negative charges diffusion on the MJS surface, facilitating the attraction between MJS and MB as a cationic dye. The observed correlation underscores the significance

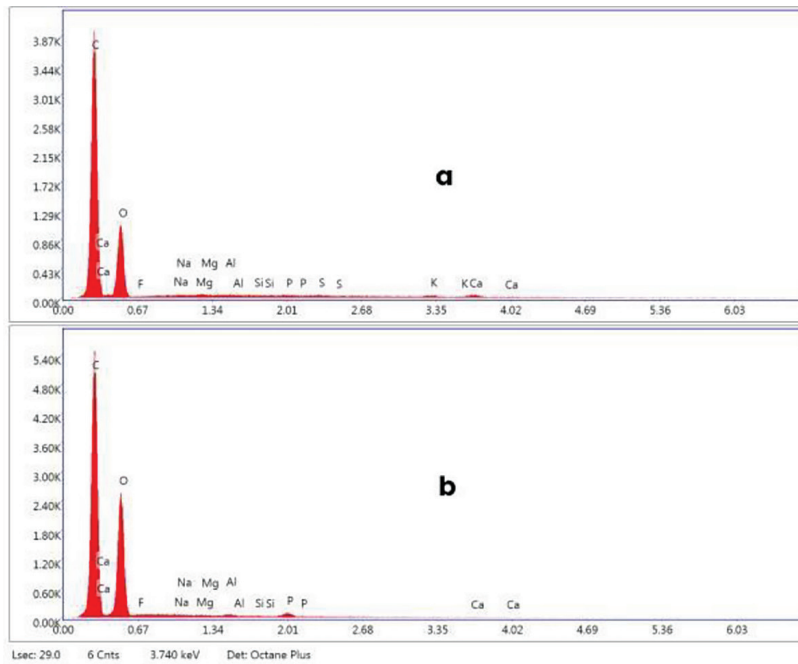


Figure 3. EDX of the JS (a) and MJS (b)

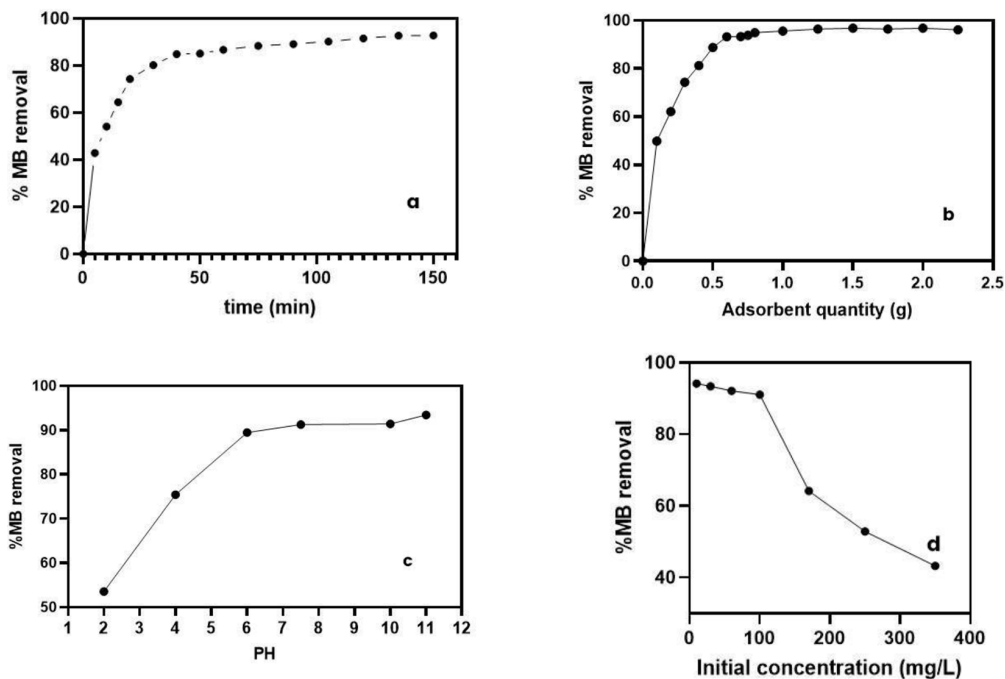
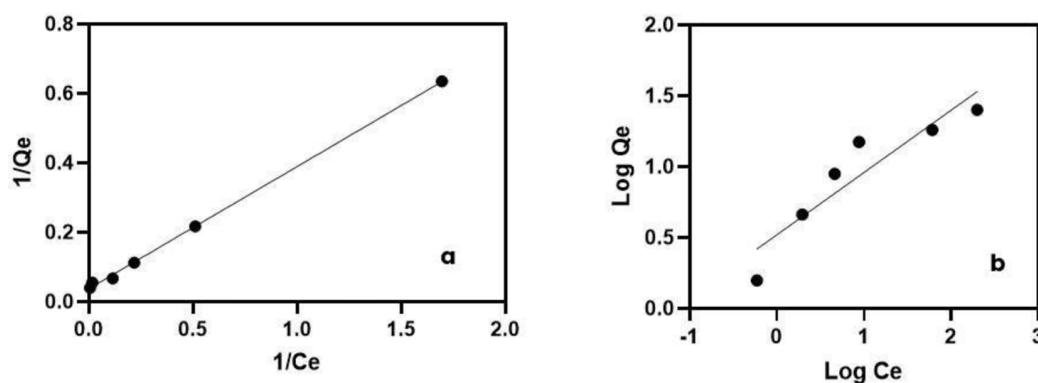


Figure 4. (a) Contact time; (b) adsorbent amount effect ; (c) pH ; (d) initial dye concentration on MB adsorption



**Figure 5.** Adsorption isotherms of MB at the surface of MJS: (a) Langmuir isotherms; (b) Freundlich isotherms

of pH control in enhancing the adsorption process for effective removal of MB using MJS as the adsorbent (Said et al., 2023).

#### Effect of MB initial concentration

The investigation into the effect of concentration ranging from 10 to 350 mg/L reveals intriguing findings. As depicted in Figure 4d, there is a notable decrease in the percentage of adsorption, plummeting from an impressive 94% down to 43%. The decrease is attributed to the saturation of adsorption sites within the adsorbent material. As the concentration of methylene blue increases, the available sites for adsorption become increasingly occupied, resulting in a diminishing capacity for further adsorption. This observation underscores the importance of optimizing the concentration of the dye in wastewater treatment processes to achieve the highest efficiency of the adsorption process (Arenas et al., 2023).

#### Adsorption isotherms

To assess the impact of initial MB concentration on adsorption, the study utilized concentration effects to analyze Langmuir and Freundlich isotherms. The Langmuir model, expressed in its linearized form (Eq. 3), suggests homogeneous adsorption occurring on the surface sites of the adsorbent. This model assumes monolayer adsorption, with adsorbate molecules evenly distributed on available surface sites without interaction between neighboring molecules (Mahdi, 2023). By applying these isotherm models, valuable insights are gained into the adsorption behavior of MB onto the adsorbent material across various initial concentration levels, aiding in the optimization of adsorption systems for practical applications.

$$\frac{1}{Q_e} = \frac{1}{Q_{max} K_L C_e} + \frac{1}{Q_{max}} \quad (3)$$

where:  $Q_{max}$  is the maximum capacity of adsorption (mg/g) of MB using the Langmuir model,  $C_e$  represents the MB concentration at equilibrium (mg/L),  $k_L$  is the Langmuir isotherm constant. The separation factor ( $R_L$ ) was also identified using equation (4) where  $C_0$  is the initial MB concentration (mg/L):

$$R_L = \frac{1}{1 + K_L C_0} \quad (4)$$

The  $R_L$  values offer valuable insights into the characteristics of adsorption mechanisms. A range of 0 to 1 for  $R_L$  indicates a favorable adsorption condition, while  $R_L$  equaling 1 indicates a linear relationship. Values exceeding 1 suggest unfavorable adsorption, implying capacity limitations of the adsorbent. In contrast,  $R_L$  equaling 0 denotes irreversible adsorption, where saturation or irreversible binding occurs (Muhammad et al., 2023). The Freundlich model is a widely used framework for describing the adsorption process of dyes onto heterogeneous surfaces of adsorbents (Gülen and Deler, 2024). It posits that the concentration of adsorbate on the adsorbent surface increases with the adsorbate amount in the solution. This model provides valuable insights into the non-ideal and multilayered nature of adsorption phenomena. The linearized form of the Freundlich equation, described by equation (5), facilitates the analysis and interpretation of experimental data, allowing researchers to quantify the adsorption behavior and characterize the affinity between the adsorbate and adsorbent (Rudram et al., 2024).

$$\log Q_e = \log K_F + \frac{1}{n} \log C_e \quad (5)$$

The Freundlich isotherm constant  $K_F$  serves as an important indicator of the adsorbent's

adsorption capacity, typically measured in mmol/g. This parameter reflects the adsorbent’s ability to capture adsorbate molecules from the solution. Meanwhile, 1/n value below 1 suggests a favorable adsorption process, with lower values indicating higher favorability (Debnath and Das, 2023). The experimental data suggests that the adsorption behavior of MB on MJS conforms to the Langmuir model, as evidenced by the higher correlation coefficients presented in Table 2. The adsorption capacity (Q<sub>max</sub>) takes a maximum of 26.52 mg/g for MJS. Furthermore, the separation factor (R<sub>L</sub>), lying between 0 and 1, signifies a favorable adsorption process of MB onto MJS under the specific experimental conditions. Furthermore, the n values, which measure the favorability of the adsorption process, indicate favorable adsorption when 0 < n < 10, further validating the efficiency of MJS as an adsorbent for MB removal (Bellaj et al., 2024; Nasiri et al., 2024)

### Adsorption kinetics

In the study of adsorption processes, the application of pseudo first and second-order models has been instrumental. The pseudo first-order model simplifies the analysis by assuming that the rate of adsorption is solely contingent on the concentration of MB, with MJS in excess or maintaining a relatively constant concentration. This model offers a straightforward approach to understanding the kinetics of the adsorption process, facilitating a thorough exploration of the various factors and mechanisms at play in the phenomenon of adsorption. Expanding on this, the pseudo second-order model considers the interaction between MB and MJS, providing a more comprehensive representation of the adsorption kinetics. Equations 6 and 7 represent the mathematical formulations for kinetic models, pseudo first and second-order,

respectively, commonly used in adsorption studies (Mohamed et al., 2024; Velarde et al., 2024).

$$\log(Q_e - Q_t) = \log Q_e - \frac{K_1 \cdot t}{2,303} \quad (6)$$

$$\frac{t}{Q_t} = \left(\frac{1}{Q_e}\right) \cdot t + \frac{1}{K_2 Q_e^2} \quad (7)$$

In adsorption studies, Q<sub>e</sub> and Q<sub>t</sub> represent the capacity at equilibrium and at time, measured in (mg/g), respectively. The parameter K<sub>1</sub> signifies the rate constant of the pseudo-first-order model, denoting the rate at which adsorption approaches equilibrium (1/min). While, K<sub>2</sub> represents the pseudo-second-order rate constant in (g/mg min). These parameters play important roles in understanding the kinetics of adsorption processes, promoting the adsorption systems optimization for a range of industrial and environmental applications.

Figure 6 and Table 4 present compelling evidence supporting the fit to the adsorption process of the pseudo-second-order model. The R<sup>2</sup> values from this model are displayed in table 4 indicate a pronounced relationship between the experimental and calculated results, suggesting a close agreement between the observed and predicted data. Moreover, Table 4 reveals that the experimental adsorption capacity (Q<sub>e</sub>) closely aligns with the calculated Q values derived out of pseudo-second-order model, further validating the model suitability for describing the adsorption kinetics (Nayl et al., 2023; Zein et al., 2023)

### Temperature effect and thermodynamic study

An investigation into the adsorption of MB onto MJS was conducted over the studied range of temperatures. Throughout the experiments, the adsorbent dosage remained constant at 0.6g, while the pH was maintained at 7.5, and the initial MB concentration stood at 15 mg/l. Thermodynamic parameters including entropy (ΔS, kJ/mol·K), standard enthalpy (ΔH, kJ/mol), and

**Table 2.** Isotherm parameters for MB removal by MJS

Langmuir			Freundlich		
R <sup>2</sup>	k <sub>L</sub> (L/mg)	Q <sub>max</sub> (mg/g)	R <sup>2</sup>	n (mg/g)	K <sub>F</sub>
0.9996	0.1072	26.5252	0.8556	2.275	3.306

**Table 3.** The R<sub>L</sub> factor at different MB concentration

C <sub>0</sub> (mg /l)	10	30	60	100	170	350
R <sub>L</sub> values	0.4817	0.2398	0.1259	0.0854	0.0520	0.0260

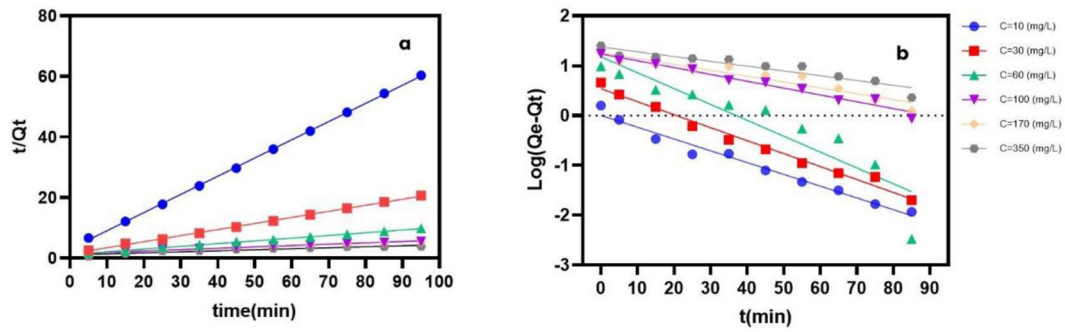


Figure 6. Kinetic adsorption of MB onto MJS: (a) pseudo-second-order kinetics; (b) pseudo-first-order

Table 4. Kinetics study at different concentrations ( $C_0$ ) for the adsorption of MB using MJS

$C_0$ (mg/l)	$Q_e$ exp (mg/g)	Pseudo-second order kinetics			Pseudo-first order kinetics		
		$Q_e$ cal (mg/g)	$K_2$	$R^2$	$Q_e$ cal (mg/g)	$K_1$ (/min)	$R^2$
10	1.58	1.66	0.1195	0.9997	0.93	0.0550	0.9216
30	4.60	3.74	0.0507	0.9988	1.13	0.0599	0.9854
60	8.90	8.71	0.0047	0.9832	11.57	0.0530	0.8414
100	14.91	13.85	0.0032	0.9988	18.29	0.0486	0.9036
170	18.18	16.58	0.0028	0.9997	13.21	0.0274	0.9585
350	25.20	22.27	0.0020	0.9516	18.78	0.0258	0.9107

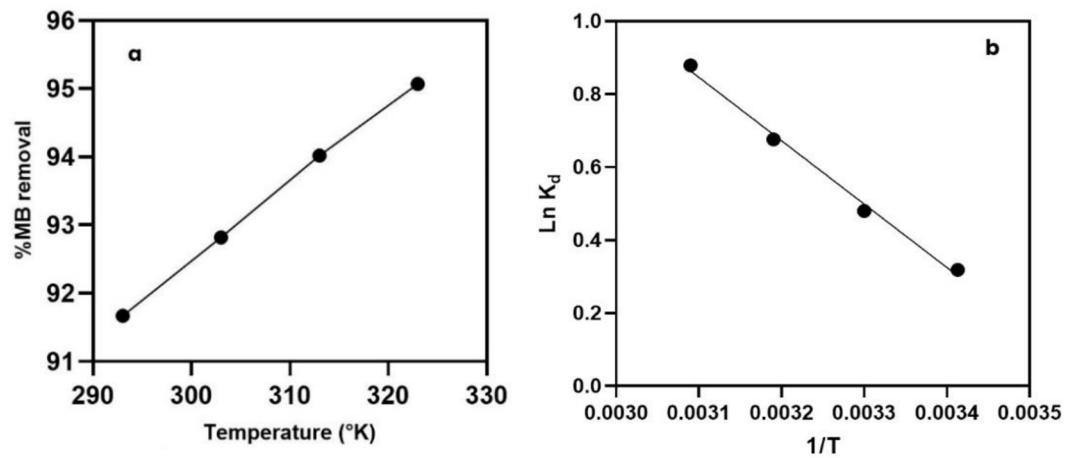


Figure 7. (a) Temperature effect on MB adsorption into MJS; (b) plot  $\ln(K_d)$  vs  $1/T$

free energy ( $\Delta G$ , kJ/mol) were determined using equations 8, 9, and 10 respectively. These analyses provide shed light on adsorption process energetics, enhancing the understanding of MB and MJS interaction across varying temperatures (Yussuff et al., 2024).

$$K_d = \frac{c_a}{c_e} \quad (8)$$

$$\ln K_d = \frac{-\Delta H}{RT} + \frac{\Delta S}{R} \quad (9)$$

$$\Delta G = -RT \ln K_d \quad (10)$$

$R$  is the gas constant in J/mol while  $T$  is the absolute temperature in Kelvin. The distribution coefficient at equilibrium  $K_d$  measured in ml/g, reflects adsorbate distribution between the solid and liquid phases at equilibrium. These parameters provide valuable insights into the affinity and interactions between MB and MJS.

Figure 7a illustrates while the temperature rises, the adsorption capacity rises, attaining 94.9% at 60 °C. The adsorption process of MB utilizing MJS demonstrates feasibility and spontaneity, evident from the negative values of  $\Delta G$  (Karami et al.,

**Table 5.** Thermodynamic insights into MB removal by MJS

$T^{\circ}$	$\Delta S$ (J/mol.K)	$\Delta G$ (KJ/mol)	$\Delta H$ (KJ/mol)
293	52.84	-6.99	14.75
303		-11.29	
313		-16.78	
323		-22.79	

2024). The positive  $\Delta H$  values indicate an endothermic nature for the adsorption process (Wu et al., 2024). Particularly, the calculated  $\Delta H$  being less than 40 kJ/mol implies a physisorption mechanism predominates (de Santana et al., 2024). The positive change in entropy ( $\Delta S$ ) indicates a rise in the level of freedom for the adsorbed species. (Peng et al., 2024), signifying a more disordered arrangement at the MJS interface. This randomness in organization is characteristic of physical sorption, primarily occurring through electrostatic interactions (Juturu et al., 2024). These findings shed light on the thermodynamics and mechanisms governing the adsorption phenomenon between MB and MJS (Reddy et al., 2023; Sultana et al., 2022).

## CONCLUSION

In conclusion, this research has effectively developed modified jujube stones as a potent adsorbent for methylene blue removal. The adsorption process adhered to the Langmuir model, exhibiting a maximum adsorption capacity of 26.52 mg/g, indicative of monolayer adsorption on a homogeneous surface. Thermodynamic investigation further affirmed the favorable nature of the adsorption, highlighting its spontaneity and endothermic properties. Overall, these results emphasize the potential of modified jujube stones as effective solution for the efficient elimination of methylene blue from wastewater.

## REFERENCES

1. Ali, A., Chiang, Y. W., Santos, R. M. 2022. X-ray diffraction techniques for mineral characterization: A review for engineers of the fundamentals, applications, and research directions. *Minerals*, 12(2), 205.
2. Al-Tohamy, R., Ali, S. S., Li, F., Okasha, K. M., Mahmoud, Y. A.-G., Elsamahy, T., Jiao, H., Fu, Y., Sun, J. 2022. A critical review on the treatment of dye-containing wastewater: Ecotoxicological and health concerns of textile dyes and possible remediation approaches for environmental safety. *Ecotoxicology and Environmental Safety*, 231, 113160.
3. Arenas, L. R., Le Coustumer, P., Gentile, S. R., Zimmermann, S., Stoll, S. 2023. Removal efficiency and adsorption mechanisms of CeO<sub>2</sub> nanoparticles onto granular activated carbon used in drinking water treatment plants. *Science of the Total Environment*, 856, 159261.
4. Bal, G., Thakur, A. 2022. Distinct approaches of removal of dyes from wastewater: A review. *Materials Today: Proceedings*, 50, 1575–1579.
5. Bellaj, M., Aziz, K., El Achaby, M., El Haddad, M., Gebrati, L., Kurniawan, T. A., Chen, Z., Yap, P.-S., Aziz, F. 2024. Cationic and anionic dyes adsorption from wastewater by clay-chitosan composite: An integrated experimental and modeling study. *Chemical Engineering Science*, 285, 119615.
6. Benjelloun, M., Miyah, Y., Evrendilek, G. A., Zerrouq, F., Lairini, S. 2021. Recent advances in adsorption kinetic models: their application to dye types. *Arabian Journal of Chemistry*, 14(4), 103031.
7. Bouchelkia, N., Benazouz, K., Mameri, A., Belkhir, L., Hamri, N., Belkacemi, H., Zoukel, A., Amrane, A., Aoulmi, F., Mouni, L. 2023. Study and Characterization of H<sub>3</sub>PO<sub>4</sub> Activated Carbons Prepared from Jujube Stones for the Treatment of Industrial Textile Effluents. *Processes*, 11(9), 2694.
8. Bouchelta, C., Medjram, M. S., Bertrand, O., Bellat, J. P. 2008. Preparation and characterization of activated carbon from date stones by physical activation with steam. *Journal of Analytical and Applied Pyrolysis*, 82(1), 70–77.
9. Bulin, C., Xiong, Q., Zheng, R., Li, C., Ma, Y., Guo, T. 2024. High efficiency removal of methyl blue using phytic acid modified graphene oxide and adsorption mechanism. *Spectrochimica Acta Part A: Molecular and Biomolecular Spectroscopy*, 307, 123645.
10. de Santana, J. E., de Andrade, F. G. S., Ferreira, A. F., Ghislandi, M. G., & da Motta Sobrinho, M. A. 2024. Isotherms, kinetics and thermodynamics of industrial dye acid red 27 adsorption on Sugarcane Bagasse Ash. *Environmental Science and Pollution Research*, 1–15.
11. Debnath, S., Das, R. 2023. Strong adsorption of CV dye by Ni ferrite nanoparticles for waste water purification: Fits well the pseudo second order kinetic and Freundlich isotherm model. *Ceramics International*, 49(10), 16199–16215.
12. El-Shafie, A. S., Rahman, E., GadelHak, Y., Mahmoud, R., El-Azazy, M. 2024. Techno-economic assessment of waste mandarin biochar as a green adsorbent for binary dye wastewater effluents of methylene blue and basic fuchsin: Lab-and large-scale investigations. *Spectrochimica Acta Part A: Molecular and Biomolecular Spectroscopy*, 306, 123621.

13. Garg, R., Garg, R., Sillanpää, M., Alimuddin, Khan, M.A., Mubarak, N.M., Tan, Y.H. 2023. Rapid adsorptive removal of chromium from wastewater using walnut-derived biosorbents. *Scientific Reports*, 13(1), 6859.
14. Ghobadi, A., Amini-Behbahani, F., Yousefi, A., Shirazi, M. T., Behnoud, N. 2019. Medicinal and nutritional properties of *Ziziphus jujuba* Mill. in traditional persian medicine and modern phytotherapy. *Crescent Journal of Medical & Biological Sciences*, 6(2).
15. Gomes, K., Caucci, S., Morris, J., Guenther, E., Miggelbrink, J. 2024. Sustainability transformation in the textile industry—The case of wastewater management. *Business Strategy & Development*, 7(1), e324.
16. Gülen, J., Deler, Ö. 2024. The potential capability of treated perlite for removal of penta chloro nitrobenzene. *Zeitschrift für Physikalische Chemie*.
17. Hariharana, T., Gokulanb, R., Al-Zaqric, N., Waradd, I. 2023. Enhanced biosorption of hexavalent chromium ions from aqueous solution onto *Ziziphus jujube* seeds as ecofriendly biosorbent—equilibrium and kinetic studies. *Researchgate*.
18. Iwuzor, K. O., Ighalo, J. O., Ogunfowora, L. A., Adeniyi, A. G., Igwegbe, C. A. 2021. An empirical literature analysis of adsorbent performance for methylene blue uptake from aqueous media. *Journal of environmental chemical engineering*, 9(4), 105658.
19. Juturu, R., Murty, V. R., Selvaraj, R. 2024. Efficient adsorption of Cr (VI) onto hematite nanoparticles: ANN, ANFIS modelling, isotherm, kinetic, thermodynamic studies and mechanistic insights. *Chemosphere*, 349, 140731.
20. Karami, F., Shokrollahi, A., Abbasi, S. 2024. Investigation of Isotherm, Thermodynamic, and Kinetics of Bovine Serum Albumin Adsorption onto MCM-41@LDH. *Analytical and Bioanalytical Chemistry Research*, 11(2), 177–189.
21. Khan, T. A., Nouman, M., Dua, D., Khan, S. A., Alharthi, S. S. 2022a. Adsorptive scavenging of cationic dyes from aquatic phase by H<sub>3</sub>PO<sub>4</sub> activated Indian jujube (*Ziziphus mauritiana*) seeds based activated carbon: Isotherm, kinetics, and thermodynamic study. *Journal of Saudi Chemical Society*, 26(2), 101417.
22. Khan, T. A., Nouman, M., Dua, D., Khan, S. A., Alharthi, S. S. 2022b. Adsorptive scavenging of cationic dyes from aquatic phase by H<sub>3</sub>PO<sub>4</sub> activated Indian jujube (*Ziziphus mauritiana*) seeds based activated carbon: Isotherm, kinetics, and thermodynamic study. *Journal of Saudi Chemical Society*, 26(2), 101417.
23. Li, H.-Z., Zhang, Y.-N., Guo, J.-Z., Lv, J.-Q., Huan, W.-W., Li, B. 2021. Preparation of hydrochar with high adsorption performance for methylene blue by co-hydrothermal carbonization of polyvinyl chloride and bamboo. *Bioresource Technology*, 337, 125442.
24. Li, Y., Yang, J., Pan, Z., Tong, W. 2020. Nanoscale pore structure and mechanical property analysis of coal: An insight combining AFM and SEM images. *Fuel*, 260, 116352.
25. Liu, Y., Wang, S., Huo, J., Zhang, X., Wen, H. T., Zhang, D., Zhao, Y., Kang, D., Guo, W., Ngo, H. H. 2024. Adsorption recovery of phosphorus in contaminated water by calcium modified biochar derived from spent coffee grounds. *Science of The Total Environment*, 909, 168426.
26. Mahdi, N. I. 2023. Application for fitting of Langmuir and Freundlich equations Studies on the experimental data of adsorption of Methylene Blue Dye by Cobalt Oxide Surface. *Samarra Journal of Pure and Applied Science*, 5(4), 66–77.
27. Miranda, E.C., Prado, P.G., León-Velarde, C. 2024. A systematic review of polluting processes produced by the textile industry and proposals for abatement methods. *ResearchGate*.
28. Mohamed, S. M. I., Yılmaz, M., Güner, E. K., El Nemr, A. 2024. Synthesis and characterization of iron oxide-commercial activated carbon nanocomposite for removal of hexavalent chromium (Cr<sup>6+</sup>) ions and Mordant Violet 40 (MV40) dye. *Scientific Reports*, 14(1), 1241.
29. Mokhtaryan, S., Khodabakhshi, A., Sadeghi, R., Nourmoradi, H., Shakeri, K., Hemati, S., Mohammadi-Moghadam, F. 2023. New activated carbon derived from *Gundelia tournefortii* seeds for effective removal of acetaminophen from aqueous solutions: Adsorption performance. *Arabian Journal of Chemistry*, 16(11), 105253.
30. Muhammad, Y. A., Sunaryono, S., Nenohai, A. J. W. T., Zulaikah, S. 2023. Adsorption of Pb (II) by magnetite coreshell silica encapsulated alginate: Characterization, adsorption kinetics and isotherm studies. *AIP Conference Proceedings*, 2687(1).
31. Narayanan, M., Jayasundara, U. 2022. Adsorption of Methylene Blue on to Blue Water Lily Stalks.
32. Nasiri, A., Golestani, N., Rajabi, S., Hashemi, M. 2024. Facile and green synthesis of recyclable, environmentally friendly, chemically stable, and cost-effective magnetic nanohybrid adsorbent for tetracycline adsorption. *Heliyon*, 10(2).
33. Nayl, A. A., Abd-Elhamid, A. I., Arafa, W. A. A., Ahmed, I. M., AbdEl-Rahman, A. M. E., Soliman, H. M. A., Abdelgawad, M. A., Ali, H. M., Aly, A. A., Bräse, S. 2023. A Novel P@ SiO<sub>2</sub> Nano-Composite as Effective Adsorbent to Remove Methylene Blue Dye from Aqueous Media. *Materials*, 16(2), 514.
34. Nimbalkar, M. N., Bhat, B. R. 2021. Simultaneous adsorption of methylene blue and heavy metals from water using Zr-MOF having free carboxylic group. *Journal of Environmental Chemical Engineering*, 9(5), 106216.
35. Palisoc, S., Dungo, J. M., Natividad, M. 2020. Low-cost supercapacitor based on multi-walled carbon nanotubes and activated carbon derived from

- Moringa Oleifera fruit shells. *Heliyon*, 6(1).
36. Panhwar, R., Sahito, I. A., Khatri, A., Jeong, S. H. 2024. Rapid and high adsorption of methylene blue dye onto graphene coated nonwoven fabric using vacuum infusion coating. *The Journal of The Textile Institute*, 1–9.
  37. Peng, S.-Y., Lin, Y.-W., Lin, K.-L. 2024. Synthesis and characterization of ecological-nanohydroxyapatite for adsorption of Cd<sup>2+</sup>. *Materials Science and Engineering: B*, 302, 117214.
  38. Rashid, R., Shafiq, I., Akhter, P., Iqbal, M. J., Hussain, M. 2021. A state-of-the-art review on wastewater treatment techniques: the effectiveness of adsorption method. *Environmental Science and Pollution Research*, 28, 9050–9066.
  39. Rawat, B., Garg, A. P. 2021. Characterization of phytochemicals isolated from cucurbita pepo seeds using uv-vis and ftr spectroscopy. *Plant Archives* (09725210), 21(1).
  40. Reddy, Y. S., Rotte, N. K., Hussain, S., Srikanth, V. V. S. S., Chandra, M. R. 2023. Sustainable mesoporous graphitic activated carbon as biosorbent for efficient adsorption of acidic and basic dyes from wastewater: Equilibrium, kinetics and thermodynamic studies. *Journal of Hazardous Materials Advances*, 9, 100214.
  41. Regti, A., Laamari, M. R., Stiriba, S.-E., El Haddad, M. 2017. The potential use of activated carbon prepared from Ziziphus species for removing dyes from waste waters. *Applied Water Science*, 7, 4099–4108.
  42. Rudram, C., Reddy, P. D. S., Kuruva, S. K. 2024. Fluoride removal from aqueous solution using thermally treated dolomite powder as adsorbent. *Materials Today: Proceedings*.
  43. Sahoo, S., Goswami, S. 2024. Theoretical framework for assessing the economic and environmental impact of water pollution: A detailed study on sustainable development of India. *Journal of Future Sustainability*, 4(1), 23–34.
  44. Said, H. A., Bourhim, I. A., Ouarga, A., Iraola-Arregui, I., Lahcini, M., Barroug, A., Noukrati, H. 2023. Sustainable phosphorylated microcrystalline cellulose toward enhanced removal performance of methylene blue. *International Journal of Biological Macromolecules*, 225, 1107–1118.
  45. Saning, A., Thanachayanont, C., Suksai, L., Watcharin, W., Techasakul, S., Chuenchom, L., Dechtrirat, D. 2024. Green magnetic carbon/alginate biocomposite beads from iron scrap waste for efficient removal of textile dye and heavy metal. *International Journal of Biological Macromolecules*, 129765.
  46. Shen, Z., Hou, D., Jin, F., Shi, J., Fan, X., Tsang, D. C. W., Alessi, D. S. 2019. Effect of production temperature on lead removal mechanisms by rice straw biochars. *Science of the Total Environment*, 655, 751–758.
  47. Shende A., Chidambaram R. 2024. Microwave-assisted synthesis, characterization, and application of tragacanth gum grafted copolymer as bioflocculant for the treatment of textile wastewater using coagulation-flocculation technique: Swelling behavior and biodegradation studies. *Journal of Applied Polymer Science*, e55247.
  48. Sher, F., Iqbal, S. Z., Albazzaz, S., Ali, U., Mortari, D. A., Rashid, T. 2020. Development of biomass derived highly porous fast adsorbents for post-combustion CO<sub>2</sub> capture. *Fuel*, 282, 118506.
  49. Sultana, S., Islam, K., Hasan, M. A., Khan, H. M. J., Khan, M. A. R., Deb, A., Al Raihan, M., Rahman, M. W. 2022. Adsorption of crystal violet dye by coconut husk powder: isotherm, kinetics and thermodynamics perspectives. *Environmental Nanotechnology, Monitoring & Management*, 17, 100651.
  50. Velarde, L., Nikjoo, D., Escalera, E., Akhtar, F. 2024. Bolivian natural zeolite as a low-cost adsorbent for the adsorption of cadmium: Isotherms and kinetics. *Heliyon*, 10(1).
  51. Venkatesan, S., Suresh, S., Arumugam, J., Ramu, P., Pugazhenthiran, N., Jothilakshmi, R., Prabu, K. M. 2024. Sunlight assisted degradation of methylene blue dye by zinc oxide nanoparticles green synthesized using Vitex negundo plant leaf extract. *Results in Chemistry*, 7, 101315.
  52. Vidaarth, T. M. N., Surendhiran, S., Jagan, K. S. G., Savitha, S., Balu, K. S., Karthik, A., Kalpana, B. 2024. Surface chemistry of phytochemical enriched MgO nanoparticles for antibacterial, antioxidant, and textile dye degradation applications. *Journal of Photochemistry and Photobiology A: Chemistry*, 448, 115349.
  53. Wu, H., Qin, J., Ji, W., Palupi, N. W., Yang, M. 2024. Interaction between curcumin and ultrafiltered casein micelles or whey protein, and characteristics of their complexes. *Journal of Food Science*.
  54. Yang, P., Lu, Y., Zhang, H., Li, R., Hu, X., Shahab, A., Elnaggar, A. Y., Alrefaei, A. F., Almutairi, M. H., Ali, E. 2024. Effective removal of methylene blue and crystal violet by low-cost biomass derived from eucalyptus: Characterization, experiments, and mechanism investigation. *Environmental Technology & Innovation*, 33, 103459.
  55. Yusuff, A. S., Gbadamosi, A. O., Bode-Olajide, F. B., Igbafe, A. I. 2024. Adsorption of methyl ester sulfonate surfactant on Berea sandstone: parametric optimization, kinetics, isotherm and thermodynamics studies. *Colloids and Surfaces A: Physicochemical and Engineering Aspects*, 133363.
  56. Zein, R., Purnomo, J. S., Ramadhani, P., Alif, M. F., Putri, C. N. 2023. Enhancing sorption capacity of methylene blue dye using solid waste of lemongrass biosorbent by modification method. *Arabian Journal of Chemistry*, 16(2), 104480.